



Cite this: *Lab Chip*, 2025, **25**, 2722

Understanding the role of vascular stretch on modulation of VWF and ANGPT-2 in continuous flow left ventricular assist device (CF-VAD) patients†

Jay Prakash Sah,^{ab} Javier E. Dominguez De Leon, ^{ab} Ian C. Berg,^{ab} Braden L. Cornelius,^{ab} Daniel B. Dekle,^{ab} Esraa Ismail, ^{ab} Xuanhong Cheng, ^{cd} Guruprasad A. Giridharan^e and Palaniappan Sethu ^{ab}^{*}

Non-surgical bleeding is a common complication in patients on continuous flow left ventricular assist device (CF-VAD) support. This study investigates how the transition from cyclic to constant stretch following CF-VAD implantation affects endothelial biosynthesis and release of Von Willebrand factor (VWF) and angiopoietin-2 (ANGPT-2), two molecules that play an essential role in the development of non-surgical bleeding. Human aortic endothelial and umbilical vein endothelial cells (HAECs and HUVECs) were cultured within a uniaxial stretch device that mimics stretch associated with both normal pulsatile and CF-VAD conditions. Following 72 hours of stretch, transcriptional regulation, intracellular accumulation, and secretion of VWF and ANGPT-2 were evaluated using molecular expression profiling and immunofluorescence microscopy. Constant stretch associated with CF-VADs upregulates transcriptional levels of VWF and ANGPT-2 in HAECs and HUVECs compared to physiological cyclic stretch ($p < 0.05$). Transcriptional increases in both VWF and ANGPT-2 in HAECs also resulted in increased intracellular protein levels of VWF and ANGPT-2 measured using ELISA, western blots and immunofluorescence microscopy, whereas in HUVECs, the intracellular increase was evident only with western blots and immunofluorescence microscopy. Finally, constant stretch appears to promote ANGPT-2 release and inhibit release of VWF from both HAECs and HUVECs compared to cyclic stretch. Our study found that constant stretch upregulates the production of both VWF and ANGPT-2. However, while the release of ANGPT-2 is elevated under constant stretch, the release of VWF declines, resulting in elevated extracellular levels of ANGPT-2, but not VWF.

Received 15th December 2024,
Accepted 25th April 2025

DOI: 10.1039/d4lc01065e
rsc.li/loc

Introduction

Continuous flow left ventricular assist devices (CF-VADs) are the gold standard for patients with advanced heart failure (HF) refractory to medical therapy, and an essential bridge

therapy for transplant-eligible individuals.¹ Despite providing circulatory support and significantly improving the survival of HF patients, CF-VADs are associated with device-related complications, particularly gastrointestinal (GI) bleeding and the formation of arteriovenous malformations (AVMs), which remain common and negatively affect the recovery and quality of life in HF patients.²

Despite a strong correlation between continuous flow and GI bleeding, the exact mechanisms *via* which the change from normal pulsatile flow to continuous flow contributes to the development of GI bleeding are poorly understood. Two molecules that play important roles in the development of GI bleeding are angiopoietin-2 (ANGPT-2) and von Willebrand factor (VWF). Evaluation of blood samples from CF-VAD patients by our group and others has shown that patients on CF-VAD support experience elevated circulating levels of ANGPT-2,^{3,4} and decreased circulating levels of VWF.^{3,5-12} More importantly, circulating VWF in CF-VAD patients is

^a Division of Cardiovascular Disease, Heersink School of Medicine, The University of Alabama at Birmingham, Birmingham, Alabama, USA.

E-mail: psethu@uabmc.edu; Tel: +1 205 975 1697

^b Department of Biomedical Engineering, School of Engineering and School of Medicine, The University of Alabama at Birmingham, Birmingham, Alabama, USA

^c Department of Bioengineering, Lehigh University, Bethlehem, Pennsylvania, USA

^d Department of Bioengineering and Materials Science and Engineering, Lehigh University, Bethlehem, Pennsylvania, USA

^e Department of Bioengineering, J. B. Speed School of Engineering, University of Louisville, Louisville, Kentucky, USA

† Electronic supplementary information (ESI) available. See DOI: <https://doi.org/10.1039/d4lc01065e>



degraded into low molecular weight (MW) fragments that are inefficient in facilitating coagulation.^{12–14} While VWF degradation has been attributed to the high shear associated with the CF-VAD impeller, the underlying mechanisms that contribute to changes in circulating levels of ANGPT-2 and VWF (*i.e.* production and release) are not known.

Endothelial cells that make up the vascular network are highly mechanosensitive.^{15,16} Under normal physiological conditions, the vascular endothelium experiences pulsatile flow which results in the imposition of cyclic shear stress and stretch. Pulsatility is very prominent in arterial vessels and decreases in capillaries and venous vessels. Arterial pulse pressure is ~40 mm Hg whereas capillaries and veins experience pulse pressures of ~10 and 4 mmHg respectively. The compliance of venous vessels is ~20–30 mm Hg greater than arterial vessels.¹⁷ Therefore, despite significantly lower pulse pressures, stretch associated with arterial and venous vessels is comparable and within the physiological range of 5–15%. Following CF-VAD placement, cyclic stretch experienced across the entire vascular network is replaced by constant stretch due to the continuous flow associated with CF-VADs, which could have important consequences for the transcriptional regulation of various factors and their release into circulation.

Cyclic stretch is a critical stimulus experienced by the vascular endothelium as a consequence of pulsatile heart function and is essential for arterial and venous endothelial cell homeostasis. In patients with CF-VADs, the change from cyclic to constant stretch potentially has profound effects that alter endothelial cell signaling, particularly in the context of non-surgical bleeding. In this study, we hypothesized that the change from cyclic to constant stretch potentially contributes to differential regulation of factors involved in GI bleeding including VWF and ANGPT-2. Using a platform that allows for modeling the transition from cyclic stretch associated with normal pulsatile flow to constant stretch associated with CF-VAD flow, we sought to determine how transcription, translation, and release of VWF and ANGPT-2 are affected. To model both the arterial and venous endothelium we used human aortic endothelial cells (HAECS) and human umbilical vein endothelial cells (HUEVCs) to evaluate how different stretch conditions affected the biosynthesis and release of VWF and ANGPT-2 in arteries and veins. To accurately model what occurs in CF-VAD patients, we began by culturing endothelial cells under pulsatile stretch seen with normal heart function. Subsequently, we model CF-VAD implantation by transitioning the mode of stretch from cyclic to continuous stretch and maintain the levels of stretch at levels similar to that observed *in vivo* in arterial and venous vessels. By studying stretch in isolation from shear stress, we seek to identify the contribution of pure stretch in differentially regulating production and release of VWF and ANGPT-2 from HAECS and HUEVCs.

Materials and methods

Characterization of stretch

Stretch characteristics of the devices used to culture cells were modeled to determine the levels of vacuum needed to be applied to generate physiological levels of stretch. Modeling was accomplished using finite element analysis (FEA) in SolidWorks. For detailed methods, please see ESI† Methods.

Fabrication of stretch devices

The devices used to subject HAECS and HUEVCs to either cyclic or constant stretch were fabricated using soft lithography techniques established in our lab.¹⁸ The stretch devices consist of a thin membrane bonded to a frame to ensure the localization of cells to the central portion of the device. The thin membrane is irreversibly bonded to a well to hold the culture medium. For detailed methods, please see ESI† Methods.

Stretch device manufacturing

The stretch device components were fabricated with a biocompatible polydimethylsiloxane (PDMS; QSil 216a & 216b, CHT, Tubingen, Germany) polymer and bonded with a water-tight seal using cold plasma surface cleaning followed by a low-temperature anneal. The PDMS polymer was prepared using protocols described previously.^{3,19} The outer frame was made by pouring PDMS into a mold with 46 mm × 46 mm × 11 mm ($L \times W \times H$) dimensions and a centered circular chamber with a diameter of 26 mm. The cell-seeding chamber was fabricated with the same PDMS ratio, poured into a mold with dimensions of 6.75 mm × 8 mm × 1 mm. Both the outer frame and cell-seeding chamber molds were cured at 70 °C for 30 min. The flexible membrane was fabricated using a 10:1.5 ratio; 4 mL of the PDMS solution was spin-coated on top of a 78.5 cm² silicon wafer, until it reached an approximate thickness of 4 mm. It was cured on a hot plate at 100 °C for 10 min. After curing, the components were cleaned and bonded using oxygen cold plasma cleaning (Plasma Cleaner PDC-001, Harrick Plasma Systems, Ithaca, NY, USA). The water-tight bond was formed under 650 mTorr pressure, 30 W, and 1 min of exposure. The components were quickly pressed together and placed on a hot plate (~100 °C) for 5 min to enhance the watertight seal. The sealing of the membrane with the outer frame and cell-seeding chamber was tested for leaks before use.

Cell culture

Primary human aortic endothelial cells (HAECS) were purchased from American Type Culture Collection (Cat#: PCS-100-011, Manassas, VA, USA) and maintained in the growth medium as described previously.³

The human umbilical vein endothelial cells (HUEVCs, ATCC) was generously provided by Dr. Mary Kathryn Sewell-



Loftin (University of Alabama at Birmingham, AL, USA) and cultured in a vascular cell basal medium (Cat#: PCS-100-041, ATCC) supplemented with endothelial cell growth kit-VEGF (Cat#: PCS 100-030, ATCC), 10% fetal bovine serum (FBS, Corning Life Science, Oneonta, NY, USA), 1% penicillin-streptomycin (Corning Life Sciences) and 0.25 μ g ml⁻¹ amphotericin B (Corning Life Science) under 5% CO₂ at 37 °C.

Seeding of endothelial cells to PDMS device

Prior to seeding, sterile PDMS stretch devices were treated with O₂ plasma for 1 min and then incubated with 15 μ l ml⁻¹ human fibronectin (Corning Life Science) for 45–60 min at 37 °C to facilitate strong cell attachment. After incubation, devices were thoroughly washed with 1× PBS to remove any poorly bound fibronectin. Approximately 0.4 × 10⁶ cells

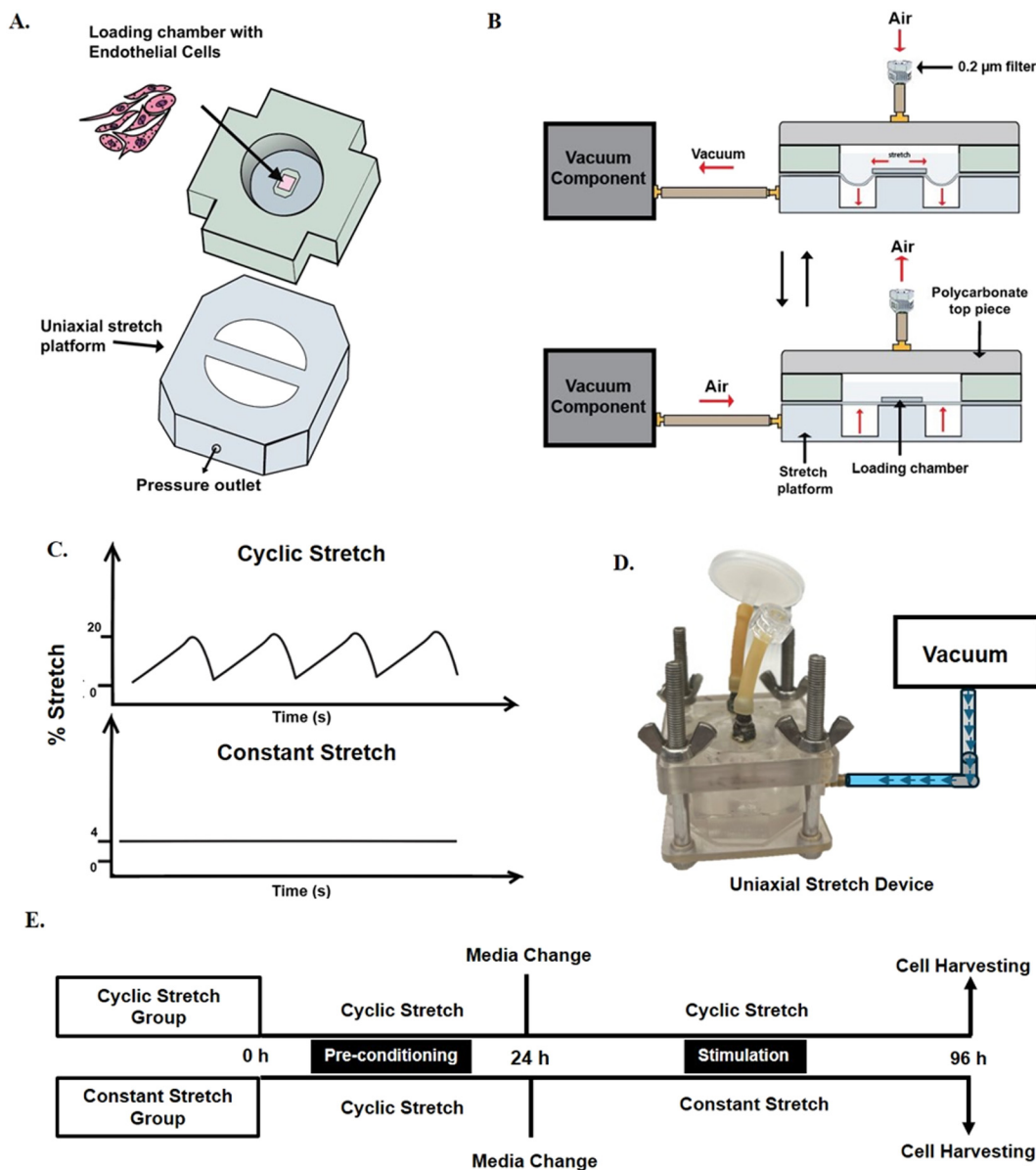


Fig. 1 (A) The schematic diagram of polydimethylsiloxane (PDMS) mold with centrally designated rectangular area for cell seeding, and uniaxial stretch platform that creates a closed chamber with the PDMS mold to apply pressure in a tightly control manner to induce stretch. (B) The schematic sketch of the working principle of the uniaxial stretch device. Cyclic or constant pressure applied to the chamber causes stretching of PDMS membrane by pushing the membrane upward. (C) Stretch and time waveforms corresponding to the stretch model. (D) The front view of PDMS uniaxial stretch device, functioning as a complete setup of a tightly regulated cell culture chamber with controlled pressure. (E) Schematic illustration of stretch experiments. Vascular endothelial cells plated to confluence in a PDMS stretch device were subjected to 24 h of physiological cyclic stretch using vacuum from a pneumatic pump to provide a normal physiological environment. After that devices were shifted to cyclic or constant stretch conditions using constant or pulsatile application of vacuum for the next 72 h, and then further analysis was performed on the culture media or cells.

(HAECs or HUVECs) suspended in 60 μ L of medium were seeded into each device and allowed to attach for 1 h. After seeding, 2 ml of growth medium was added to each device and incubated at 37 °C with 5% CO₂ level for 24–48 h to achieve a confluent monolayer.

Experimental setup of stretch devices

Autoclaved components of the stretch device setup were assembled in a sterile environment (1300 Series A2 Safety Cabinet, Thermo Scientific, Waltham, MA, USA). The seeded devices were placed on top of individual vacuum chambers (Fig. 1A) and snugly assembled between polycarbonate pieces to achieve a gas-tight seal. The polycarbonate top piece was exposed to air *via* an anti-bacterial 0.2 μ m PTFE membrane syringe filter (Fisher Scientific, Hampton, NH, USA) (Fig. 1B and D) to prevent contamination. Devices were either subjected to cyclic stretch or constant stretch. On day 0, both cyclic and constant stretch devices were placed under preliminary cyclic stretch for 24 h. The growth medium was then replaced, and the devices were either maintained under cyclic stretch or switched to constant stretch (Fig. 1D) for 72 h to model conditions seen following CF-VAD placement.

Evaluation of cells following stretch experiments

Following completion of the stretch studies, the cells (HAECs and HUVECs) subjected to cyclic and constant stretch were evaluated using brightfield and immunofluorescence microscopy to determine cellular alignment and intracellular accumulation of VWF and ANGPT-2; quantitative RT-PCR was used to evaluate relative changes in VWF and ANGPT-2 expression; and Western Blots and ELISA were used to determine both intracellular and secreted levels of VWF and ANGPT-2. For detailed methods, please refer to the ESI† Methods.

Data analysis and statistical analysis

All the experiments were performed with technical replicates (as indicated in the figure legends) and data were represented as mean \pm SEM (standard error mean). GraphPad PRISM 10.2.3 software was used to perform statistical analysis and to prepare graphs. Student's unpaired *t*-test was used for comparison of *in vitro* data, and two-tailed Student's *t*-test or ANOVA was used to compare data. Two-tailed statistical significance was set at $p < 0.05$. In graphs, (*) denotes $p < 0.05$, (**) denotes $p < 0.01$, and (***) denotes $p < 0.001$.

Results

Finite element modeling of stretch and stress

To examine the effect of constant stretch on vascular endothelium after CF-VAD implantation *in vitro*, we modeled the uniaxial stretch device (Fig. 1A, B and D) using finite element analysis (FEA) through SolidWorks Simulation, as described in ESI† methods section. In Fig. S1A and B,†

stretch of the central chamber along the Z-plane (relative plane parallel to the device) is shown in mm at the peak deformation attained with each condition. Analysis of the images shows that the expected peak stretch in the continuous group is ~4%, while the expected peak stretch in the pulsatile group is 20%. Both theoretical values are within expected ranges for CF-VAD-related stretch and physiological stretch values, respectively.²⁰ Von Mises analysis depicted in Fig. S1C and D† shows that most of the stretch-induced stress is dissipated by the cell-seeding chamber, while the membrane does not experience significant stress.

Morphological changes in HAECs and HUVECs following cyclic and constant stretch

Following culture under cyclic and constant stretch conditions, we examined the morphology of HAECs and HUVECs. We found that the HAECs treated with constant stretch attained an elongated cellular morphology compared to cells subjected to cyclic stretch conditions (Fig. 2A). In contrast to HAECs, HUVECs subjected to cyclic stretch also attained an elongated morphology but cells subjected to constant stretch did not attain an elongated phenotype as seen with HAECs (Fig. 2A).

Transcriptional profiling of VWF and ANGPT-2 in HAECs and HUVECs

To determine if the type of stretch influences transcriptional levels of VWF and ANGPT-2, we evaluated relative changes in VWF and ANGPT-2 gene expression using quantitative RT-PCR following 72 h of culture under constant or cyclic stretch (Fig. 2B and C). Our results suggest that both HAECs and HUVECs subjected to constant stretch experience a statistically significant increase in gene expression associated with VWF and ANGPT-2.

Changes in protein levels of VWF and ANGPT-2 in HAECs and HUVECs

To determine whether the type of stretch promotes biosynthesis of VWF and ANGPT-2 in vascular endothelium, we subjected both HAECs and HUVECs to 72 h of either constant or cyclic stretch and evaluated intracellular levels of VWF and ANGPT-2 from cell lysates. In HAECs, constant stretch resulted in a statistically significant increase in intracellular VWF and ANGPT-2 in comparison to cyclic stretch as confirmed *via* ELISA (Fig. 3A and B) and western blotting (Fig. 3C). In HUVECs we did not observe a statistically significant difference in the expression of both VWF and ANGPT-2 under cyclic and constant stretch conditions when profiled using ELISA (Fig. 3D and E), however, western blots show a significant increase in VWF expression under continuous stretch in comparison to cyclic stretch (Fig. 3F).



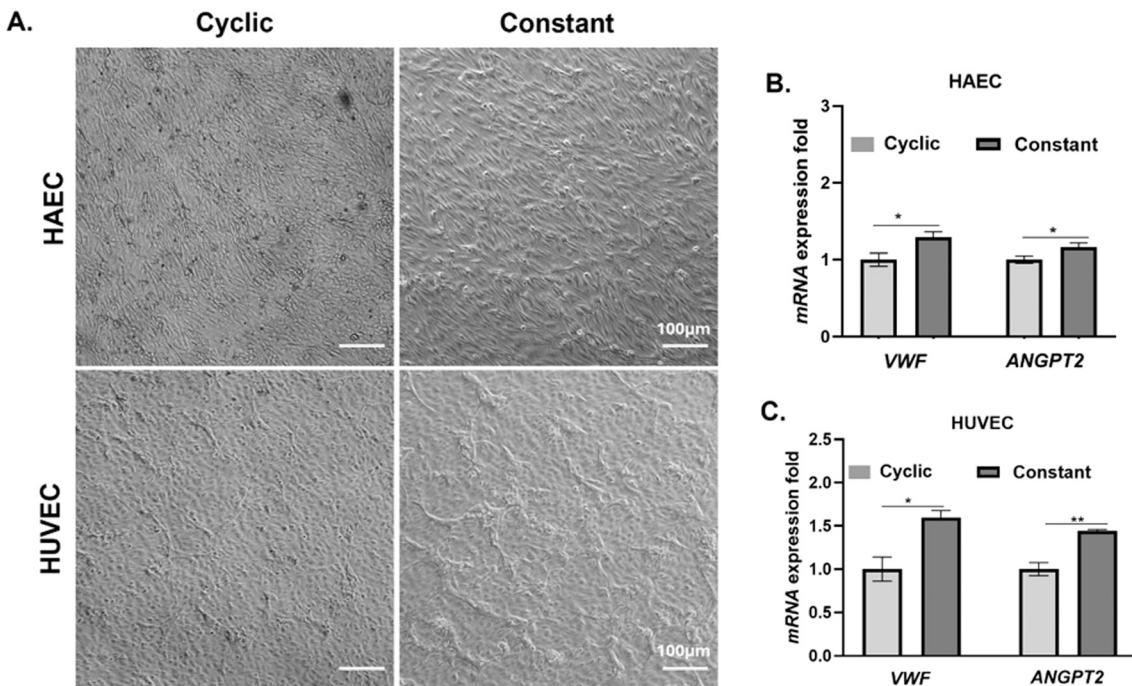


Fig. 2 (A) Phase contrast microscopic imaging (10 \times) of seeded human vascular endothelial cells (HAECs (top) or HUVECs (bottom)) within uniaxial stretch device after 72 hours of culture under cyclic or constant stretch conditions. (B and C) Changes in transcriptional levels of VWF and ANGPT-2 in HAECs (B) and HUVECs (C) after 72 h of culture under cyclic or constant stretch conditions were determined by qRT-PCR. VWF and ANGPT-2 RNA expression was normalized to β -actin expression. All experiments were performed three times with duplicate samples. Error bars indicate SEM. ***, $P < 0.001$; **, $P < 0.01$; *, $P < 0.05$.

Evaluation of intracellular VWF and ANGPT-2 in HAECs and HUVECs

Using immunofluorescence microscopy, we profiled intracellular accumulation of VWF and ANGPT-2 in HAECs and HUVECs under conditions of constant and cyclic stretch. Our results clearly show a significant increase in intracellular levels of VWF and ANGPT-2 in both HAECs and HUVECs under constant stretch when compared to cyclic stretch (Fig. 4A and B). Closer inspection of localization of VWF and ANGPT-2 suggests significant accumulation closer to the cell membrane under constant stretch in comparison to pulsatile stretch in both HAECs and HUVECs.

Release of VWF and ANGPT-2 from HAECs and HUVECs

Finally, to determine if the type of stretch influences the release of VWF and ANGPT-2 from HAECs and HUVECs into the cell culture media, we collected media from HAECs and HUVECs following 72 h of culture under constant and cyclic stretch conditions. Quantitative evaluation of secreted levels of VWF and ANGPT-2 using ELISA suggests a statistically significant decrease in secreted levels of VWF and a statistically significant increase in secreted levels of ANGPT-2 following constant stretch in comparison to cyclic stretch in HAECs (Fig. 5A and B) and in HUVECs (Fig. 5D and E). These results were further confirmed using western blot (Fig. 5C and F).

Discussion

Continuous flow left ventricular assist devices (CF-VADs) are life-saving technologies that can prolong the lifespan of individuals with advanced heart failure refractory to drugs and serve as a bridge to transplant or as destination therapy.¹ The only FDA-approved CF-VAD currently available to patients is the **Heartmate 3 (HM3)** which is a centrifugal continuous flow pump.²¹ HM3 utilizes full magnetic levitation, in which wide blood flow gaps and several design modifications to the impeller minimize friction, high shear stress and turbulence. The original HM3 uses continuous flow technology, which is associated with non-physiological flow with diminished pulsatility. The interaction of blood with the CF-VAD impeller and the loss of pulsatility, both contribute to pump thrombosis^{22,23} and non-surgical bleeding, particularly in the gastrointestinal (GI) tract.^{24,25} Design modifications to the HM3 have resulted in improved 1- and 5-year survival rates and a significant reduction in pump-related thrombosis but the incidences of bleeding remain elevated.^{26,27} Critically, despite significant technological advances and an increasing need for life saving therapies such as CF-VADs, in 2022 there were only 2464 CF-VADs implanted in the US.¹ This suggests that CF-VADs are greatly underutilized as they can potentially treat upwards of 100 000 heart failure patients a year, improve survival, and enhance their quality of life.²⁸

HM3 design modifications that minimize turbulence on blood elements and introduce intermittent sub-physiologic



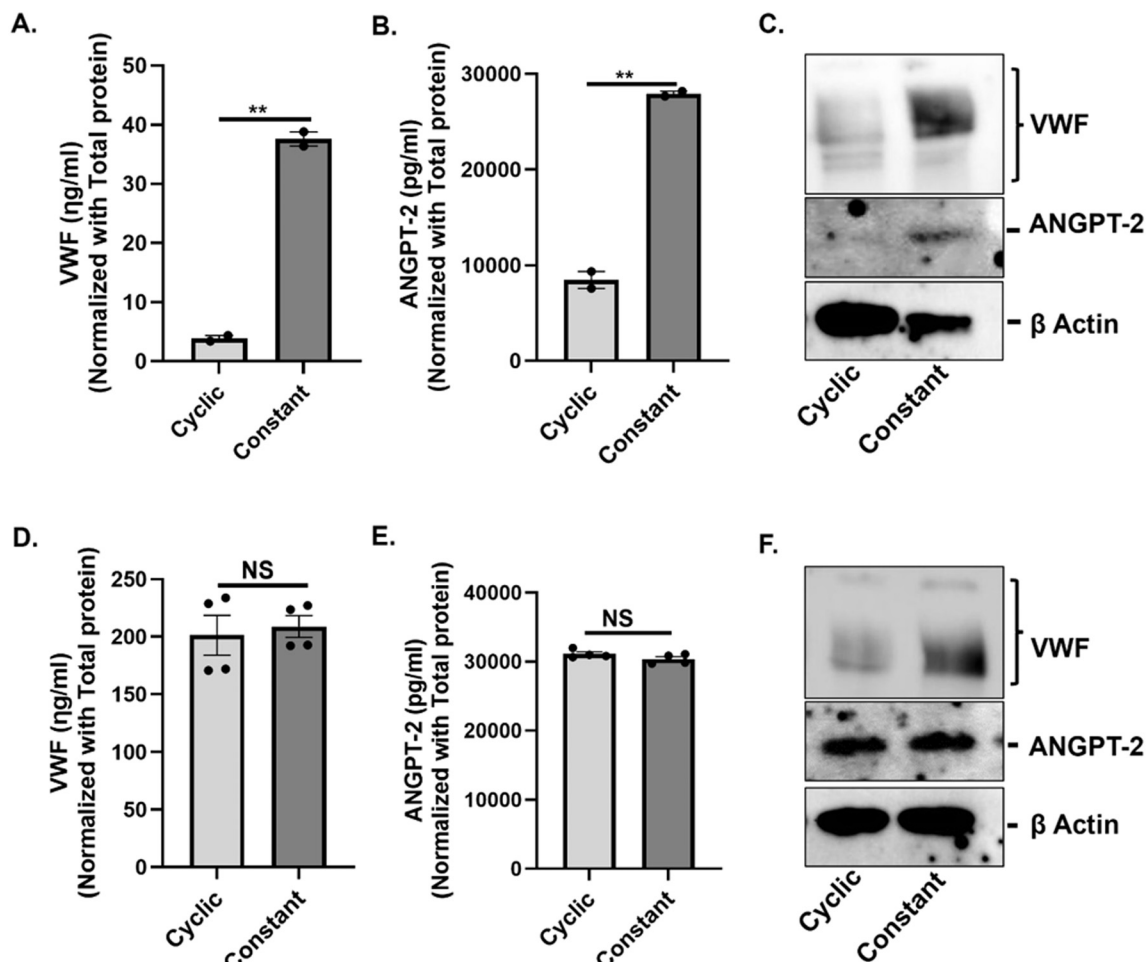


Fig. 3 (A and B) Intracellular protein levels of VWF (A) and ANGPT-2 (B) in HAECS were determined from the cell lysates after 72 h of cyclic or constant stretch treatment by ELISA. (C) Representative western blot shows the induction of intracellular VWF and ANGPT-2 in HAECS under constant stretch condition compared to cyclic stretch conditions. (D and E) The bar diagrams show the expression levels of intracellular VWF (D) and ANGPT-2 (E) in HUVECs after 72 h of cyclic or constant stretch treatment. (F) Representative western blot data show intracellular VWF and ANGPT-2 protein levels after exposure to cyclic or constant stretch conditions. All experiments were performed three times with duplicate samples. Error bars indicate SEM. ***, $P < 0.001$; **, $P < 0.01$; *, $P < 0.05$.

pulsatility have resulted in significant improvements in preventing hemolysis and thrombosis.²⁷ However, ~43% of HM3 patients developed non-surgical bleeding²⁷ suggesting that other factors away from the CF-VAD impeller may be responsible. Specifically, we were interested in pathophysiological changes in endothelial cells as a result of transition from physiological pulsatile flow to continuous flow following CF-VAD implantation. Pulsatility associated with blood flow manifests in the form of pressure, shear stress, and stretch on the endothelium.¹⁶ Pressure experienced by the compliant endothelium results in stretch on individual endothelial cells.²⁹ In this study, we sought to determine how the change from cyclic stretch associated with normal pulsatile flow to constant stretch associated with CF-VAD continuous flow affected endothelial function in the context of non-surgical bleeding.

Two molecules that have been implicated in the development of non-surgical bleeding in CF-VAD patients are ANGPT-2 and VWF.^{2-4,8,30} ANGPT-2 is a pro-angiogenic

molecule that plays a critical role in vascular remodeling and has been implicated in the development of non-surgical bleeding.^{4,31} VWF is an essential component of the coagulation cascade that bridges platelets and sub-endothelial collagen at sites of injury.^{8,32} Our group and others have profiled blood samples from CF-VAD patients and found an elevation in levels of ANGPT-2 and a decrease in VWF in circulation in these patients.³ In this study, we focused on how cyclic and constant stretch differentially regulated production and release of VWF and ANGPT-2 from endothelial cells of both arterial and venous origin.

Following 72 hours of culture under conditions of either constant or cyclic stretch, we found that constant stretch associated with CF-VADs resulted in an increase in transcriptional regulation of both ANGPT-2 and VWF in HAECS and HUVECs. The increase in gene expression subsequently resulted in increased intracellular protein levels of both ANGPT-2 and VWF as verified using ELISA, western blots and immunofluorescence microscopy. Our results

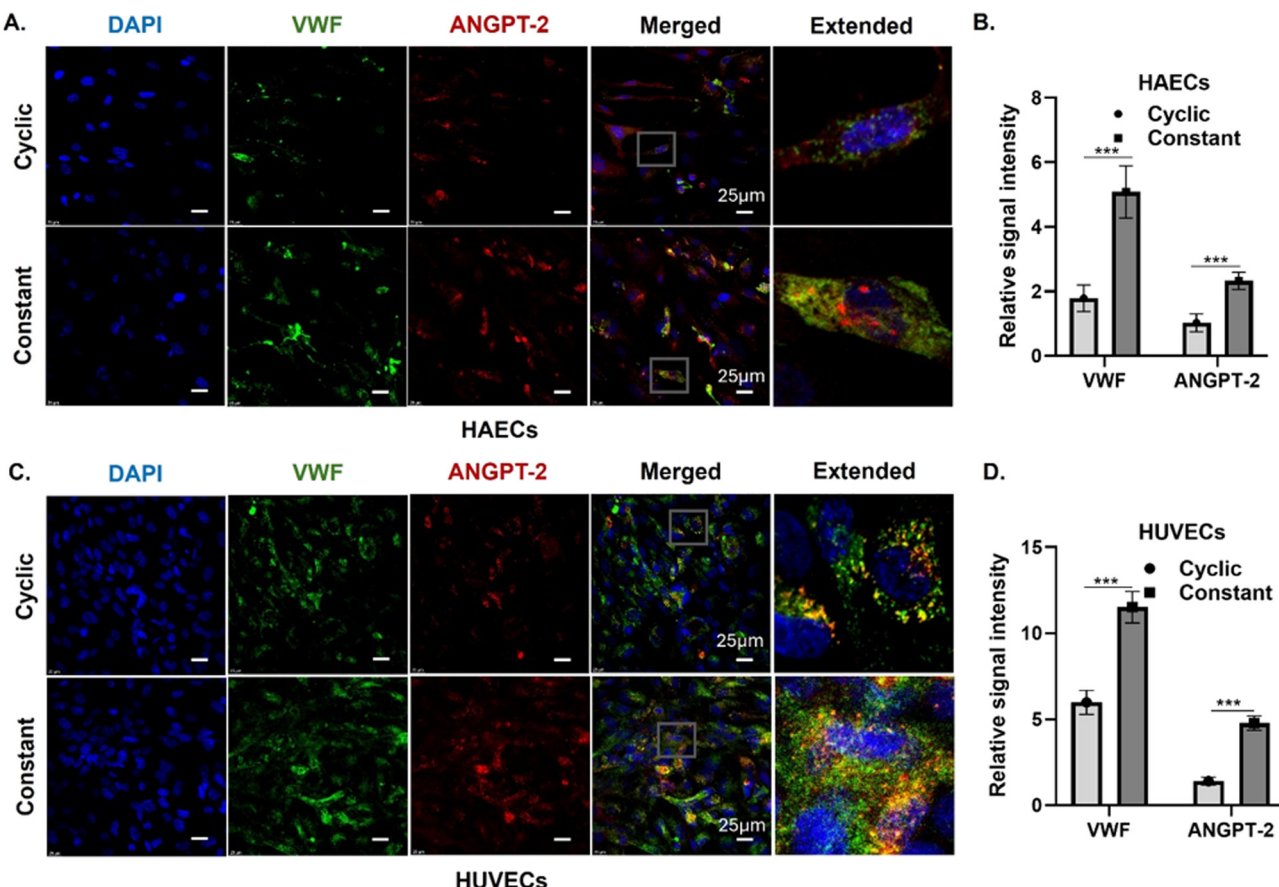


Fig. 4 (A and C) Immunofluorescence staining for VWF and ANGPT-2 expression in HAECs (A) or HUVECs (C) after 72 h of cyclic or constant stretch conditions. Cell nuclei were counterstained with DAPI. Scale bars represent 25 μ m. (B and D) The bar diagrams show the quantification of VWF or ANGPT-2 expression after 72 h of cyclic or constant stretch conditions in HAECs (B) or HUVECs (D). All experiments were performed three times with duplicate samples. Error bars indicate SEM. *** $, P < 0.001$; ** $, P < 0.01$; * $, P < 0.05$.

therefore suggest that constant stretch is a potent stimulator of ANGPT-2 and VWF gene expression resulting in enhanced translation and intracellular accumulation within both HAECs and HUVECs. Evaluation of secreted protein levels of ANGPT-2 and VWF in the culture medium however showed that ANGPT-2 level increased with constant stretch whereas VWF secretion was enhanced with cyclic stretch. In CF-VAD patients, we typically observe elevated levels of ANGPT-2 and a decline in circulating VWF levels. Our study is in agreement with clinical observations in CF-VAD patients but suggests that the decline in VWF levels is not due to suppressed transcriptional regulation but rather the inability of both HAECs and HUVECs to secrete VWF resulting in increased intracellular accumulation. Although the protein levels and their intracellular *vs.* extracellular ratios differ between HAECs and HUVECs, both cell lines exhibit the same pattern. This could be due to the distinct physiology of HUVECs, which are immortalized cells, while HAECs are primary cells and more representative of human physiology. On the other hand, the increase in transcriptional regulation of ANGPT-2 results in increases in both intracellular and secreted levels of ANGPT-2 suggesting that constant stretch does not hinder the process of ANGPT-2 secretion.

Considering the fact that the primary mechanism of release for both VWF and ANGPT-2 into circulation is *via* packaging into Weibel–Palade bodies,^{33,34} it was surprising to observe differential release of ANGPT-2 and VWF in response to cyclic and constant stretch. This can be explained by the fact that while VWF trafficking to the endothelial cell membrane for release occurs exclusively *via* Weibel–Palade bodies, several studies have shown that ANGPT-2 can also be packaged into exosomes for release into circulation.^{35–37} While both Weibel–Palade bodies and exosomes are secretory vesicles, Weibel–Palade bodies are larger and possess an elongated shape^{38,39} that can potentially affect release in response to different types of stretch.

We speculate that cyclic stretch is an essential signal for stimulation dependent release of cargo from Weibel–Palade bodies whereas, constant stretch only promotes the release of cargo contained in exosomes. Cyclic stretch likely affects the fusion of Weibel–Palade bodies to the endothelial cell membrane essential for release of stored cargo. These observations are supported by immunofluorescence imaging that shows significant accumulation of VWF and ANGPT-2 closer to the cell membrane of HAECs and HUVECs following constant stretch and not with cyclic stretch suggesting that

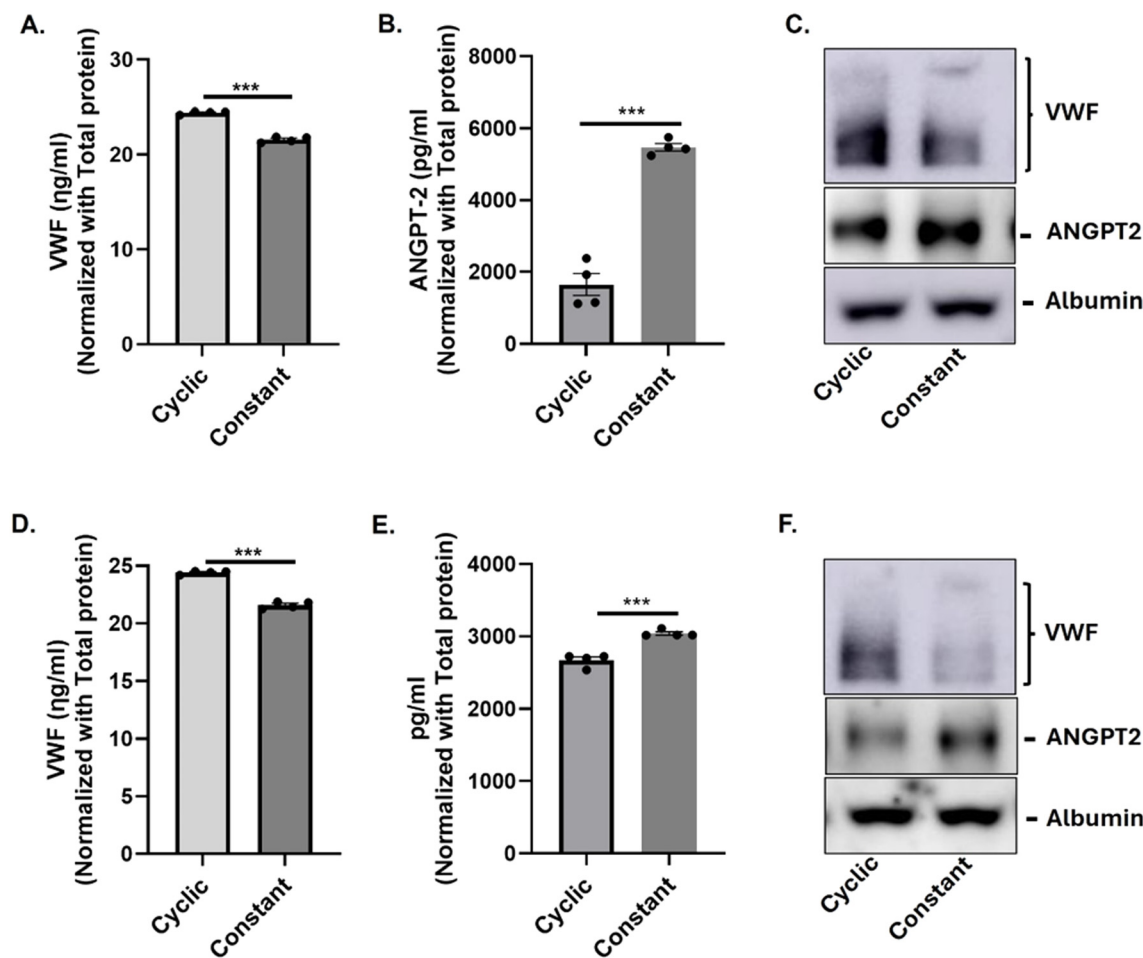


Fig. 5 (A and B) Extracellular protein levels of VWF (A) and ANGPT-2 (B) in HAECs were measured from the media collected after 72 h of cyclic or constant stretch treatment by ELISA. (C) Representative western blot data show the pattern of VWF and ANGPT2 release from HAECs under cyclic or constant stretch conditions. (D and E) The bar diagrams show the expression levels of extracellular VWF (D) and ANGPT-2 (E) in HUVECs after 72 h of cyclic or constant stretch treatment by ELISA. (F) Representative western blot data show extracellular VWF and ANGPT-2 protein levels after exposure to cyclic or constant stretch conditions. All experiments were performed three times with duplicate samples. Error bars indicate SEM. ***: $P < 0.001$; **: $P < 0.01$; *: $P < 0.05$.

VWF and ANGPT-2 packaged into Weibel–Palade bodies remain trapped within the endothelial cells under conditions of constant stretch but are efficiently released under cyclic stretch.

Other potential factors that influence differential secretion of ANGPT-2 and VWF include improper post-translational modification of VWF in the endoplasmic reticulum under conditions of constant stretch, especially defective dimerization that causes VWF to remain in its pro-VWF monomeric form, which inhibits its secretion.^{40,41} Endoplasmic reticulum (ER) stress plays an important role in pathological vascular remodeling in cardiovascular diseases.⁴² A report on the effect of homocysteine on VWF secretory mechanism suggests that ER stress contributes to an increase in intracellular VWF.⁴³ There is a possibility that continuous stretch contributes to ER stress that limits the release of VWF from endothelial cells. Finally, another report indicates that the secretion of VWF from Weibel–Palade bodies requires an elevation in intracellular Ca^{2+} levels.⁴⁴

Constant stretch potentially leads to degradation of Piezo (a mechanically activated ion channel protein), which in turn results in attenuation of calcium influx into the vascular endothelium resulting in compromised secretion.⁴⁵

Our study is the first to show that the production and secretion of ANGPT-2 and VWF are sensitive to the type of stretch (cyclic vs. constant) and that the type of stretch can play an important role in determining the circulating levels of both ANGPT-2 and VWF. Subsequent studies are necessary to determine the mechanisms associated with how the type of stretch dictates post-translational events that determine intracellular accumulation and secretion of both ANGPT-2 and VWF. While our study demonstrates the importance of the type of stretch on endothelial cells and how it may contribute to the development of non-surgical bleeding, blood flow is also associated with shear stress on the surface of endothelial cells. Therefore, results from this study need to be further validated using systems that can impose both types of stresses simultaneously.

In conclusion, this study conclusively shows that the constant stretch associated with CF-VADs results in an increase in secreted ANGPT-2 and a decrease in secreted VWF from both HAECS and HUVECS and is likely a major contributor to non-surgical bleeding. Subsequent studies are necessary to understand the exact mechanisms of how stretch affects the packaging and release of VWF and ANGPT-2 from the endothelium. Thus far, we have very limited information about how the change from cyclic to pulsatile stretch affects endothelial cell function, particularly in the context of non-surgical bleeding. Information gained from this study, specifically with regard to the production and release of VWF and ANGPT-2 from HAECS and HUVECS is novel and paves the way for targeted clinical approaches including the development of new therapeutic strategies. The use of patient-derived endothelial cells enables personalized medicine where we can model individual patient-on-a-chip and optimize operation parameters for CF-VAD devices. In a broader context, this study provides opportunities to gain mechanistic understanding of how the application of biomechanical stresses (stretch) affects endothelial signaling and how altered signaling mechanisms lead to bleeding disorders.

Data availability

Data associated with this study is available on request from the authors: the data that support the findings of this study are available from the corresponding author, PS, upon reasonable request.

Author contributions

JPS and JEDDL contributed to conceptualization, investigation, interpretation and writing – original draft. ICB, BC and DD assisted in preparing stretch devices and conducting the stretch experiments. EI assisted with the experimental design. XC and GAG provided crucial insights and feedback on the critical data and conceptual framework. PS supervised all the aspect of project, contributed to conceptualization, reviewed and edited the manuscript, and secured funding.

Conflicts of interest

There are no financial conflicts of interest related to this study.

Acknowledgements

This project was supported by a grant from the National Institute of Health (NIH) (Grant # HL151663), a grant from the National Science Foundation (NSF, 2004475), a grant from the National Science Foundation (NSF) (Grant # 2004475), and a pilot grant from the Comprehensive Cardiovascular Center at UAB.

References

- 1 M. Yuzefpolskaya, *et al.*, The Society of Thoracic Surgeons Intermacs 2022 Annual Report: Focus on the 2018 Heart Transplant Allocation System, *Ann. Thorac. Surg.*, 2023, **115**(2), 311–327.
- 2 F. W. G. Leebeek and R. Muslem, Bleeding in critical care associated with left ventricular assist devices: pathophysiology, symptoms, and management, *Hematology Am. Soc. Hematol. Educ. Program*, 2019, **2019**(1), 88–96.
- 3 K. T. Nguyen, *et al.*, von Willebrand Factor and Angiopoietin-2 are Sensitive Biomarkers of Pulsatility in Continuous-Flow Ventricular Assist Device Patients, *ASAIO J.*, 2023, **69**(6), 569–575.
- 4 C. E. Tabit, *et al.*, Elevated Angiopoietin-2 Level in Patients With Continuous-Flow Left Ventricular Assist Devices Leads to Altered Angiogenesis and Is Associated With Higher Nonsurgical Bleeding, *Circulation*, 2016, **134**(2), 141–152.
- 5 S. Takashio, *et al.*, Detection of acquired von Willebrand syndrome after ventricular assist device by total thrombus-formation analysis system, *ESC Heart Fail.*, 2020, **7**(5), 3235–3239.
- 6 G. W. Rowlands, *et al.*, PEDS15: Evaluation of vWF Degradation in the PediaFlow Fully Magnetically Levitated Pediatric Ventricular Assist Device, *ASAIO J.*, 2022, **68**(Supplement 2), 77.
- 7 I. Netuka, *et al.*, Evaluation of von Willebrand factor with a fully magnetically levitated centrifugal continuous-flow left ventricular assist device in advanced heart failure, *J. Heart Lung Transplant.*, 2016, **35**(7), 860–867.
- 8 M. Oezkun, *et al.*, Role of acquired von Willebrand syndrome in the development of bleeding complications in patients treated with Impella RP devices, *Sci. Rep.*, 2021, **11**(1), 23722.
- 9 K. Klaeske, *et al.*, Acquired von Willebrand factor deficiency is reduced in HeartMate 3 patients†, *Eur. J. Cardiothorac. Surg.*, 2019, **56**(3), 444–450.
- 10 S. Hennessy-Strahs, *et al.*, Toward a Standard Practice to Quantify von Willebrand Factor Degradation During Left Ventricular Assist Device Support, *Ann. Thorac. Surg.*, 2021, **112**(4), 1257–1264.
- 11 C. R. Bartoli, *et al.*, Pathologic von Willebrand factor degradation with a left ventricular assist device occurs via two distinct mechanisms: mechanical demolition and enzymatic cleavage, *J. Thorac. Cardiovasc. Surg.*, 2015, **149**(1), 281–289.
- 12 M. Bortot, *et al.*, Turbulent Flow Promotes Cleavage of VWF (von Willebrand Factor) by ADAMTS13 (A Disintegrin and Metalloproteinase With a Thrombospondin Type-1 Motif, Member 13), *Arterioscler., Thromb., Vasc. Biol.*, 2019, **39**(9), 1831–1842.
- 13 U. Budde, *et al.*, Detailed von Willebrand factor multimer analysis in patients with von Willebrand disease in the European study, molecular and clinical markers for the diagnosis and management of type 1 von Willebrand disease (MCDMD-1VWD), *J. Thromb. Haemostasis*, 2008, **6**(5), 762–771.



14 C. H. H. Chan, *et al.*, Discrete responses of erythrocytes, platelets, and von Willebrand factor to shear, *J. Biomech.*, 2022, **130**, 110898.

15 R. Amaya, A. Pierides and J. M. Tarbell, The Interaction between Fluid Wall Shear Stress and Solid Circumferential Strain Affects Endothelial Gene Expression, *PLoS One*, 2015, **10**(7), e0129952.

16 Y. S. Li, J. H. Haga and S. Chien, Molecular basis of the effects of shear stress on vascular endothelial cells, *J. Biomech.*, 2005, **38**(10), 1949–1971.

17 C. Gopalan and E. Kirk, *The blood vessels, in Biology of Cardiovascular and Metabolic Diseases*, ed. C. Gopalan and E. Kirk, Academic Press, 2022, ch. 2, pp. 35–51.

18 V. Parichehreh, *et al.*, Microfluidic inertia enhanced phase partitioning for enriching nucleated cell populations in blood, *Lab Chip*, 2013, **13**(5), 892–900.

19 M. Meki, *et al.*, Effects of Pulsatility on Arterial Endothelial and Smooth Muscle Cells, *Cells Tissues Organs*, 2023, **212**(3), 272–284.

20 G. Gawlak, *et al.*, Chronic high-magnitude cyclic stretch stimulates EC inflammatory response via VEGF receptor 2-dependent mechanism, *Am. J. Physiol.*, 2016, **310**(11), L1062–L1070.

21 M. N. Belkin, *et al.*, Physiology and Clinical Utility of HeartMate Pump Parameters, *J. Card. Failure*, 2022, **28**(5), 845–862.

22 Z. Chen, *et al.*, Flow features and device-induced blood trauma in CF-VADs under a pulsatile blood flow condition: A CFD comparative study, *Int. J. Numer. Methods Biomed. Eng.*, 2018, **34**(2), e2924.

23 K. H. Fraser, *et al.*, A quantitative comparison of mechanical blood damage parameters in rotary ventricular assist devices: shear stress, exposure time and hemolysis index, *J. Biomech. Eng.*, 2012, **134**(8), 081002.

24 Z. Chen, *et al.*, Non-physiological shear stress-induced blood damage in ventricular assist device, *Med. Nov. Technol. Devices*, 2019, **3**, 100024.

25 K. Cushing and V. Kushnir, Gastrointestinal Bleeding Following LVAD Placement from Top to Bottom, *Dig. Dis. Sci.*, 2016, **61**(6), 1440–1447.

26 I. Netuka, *et al.*, Evaluation of von Willebrand factor with a fully magnetically levitated centrifugal continuous-flow left ventricular assist device in advanced heart failure, *J. Heart Lung Transplant.*, 2016, **35**(7), 860–867.

27 M. R. Mehra, *et al.*, A Fully Magnetically Levitated Left Ventricular Assist Device — Final Report, *N. Engl. J. Med.*, 2019, **380**(17), 1618–1627.

28 E. J. Molina, *et al.*, The Society of Thoracic Surgeons Intermacs 2020 Annual Report, *Ann. Thorac. Surg.*, 2021, **111**(3), 778–792.

29 N. F. Jufri, *et al.*, Mechanical stretch: physiological and pathological implications for human vascular endothelial cells, *Vasc. Cell*, 2015, **7**, 8.

30 A. M. Randi, K. E. Smith and G. Castaman, von Willebrand factor regulation of blood vessel formation, *Blood*, 2018, **132**(2), 132–140.

31 R. G. Akwii, *et al.*, Role of Angiopoietin-2 in Vascular Physiology and Pathophysiology, *Cells*, 2019, **8**(5), 471.

32 Z. M. Ruggeri, The role of von Willebrand factor in thrombus formation, *Thromb. Res.*, 2007, **120**(Suppl 1), S5–S9.

33 G. Mobayen, *et al.*, von Willebrand factor binds to angiopoietin-2 within endothelial cells and after release from Weibel-Palade bodies, *J. Thromb. Haemostasis*, 2023, **21**(7), 1802–1812.

34 M. Schillemans, *et al.*, Exocytosis of Weibel-Palade bodies: how to unpack a vascular emergency kit, *J. Thromb. Haemostasis*, 2019, **17**(1), 6–18.

35 R. Ju, *et al.*, Angiopoietin-2 secretion by endothelial cell exosomes: regulation by the phosphatidylinositol 3-kinase (PI3K)/Akt/endothelial nitric oxide synthase (eNOS) and syndecan-4/syntenin pathways, *J. Biol. Chem.*, 2014, **289**(1), 510–519.

36 J. Y. Xie, *et al.*, Angiopoietin-2 induces angiogenesis via exosomes in human hepatocellular carcinoma, *Cell Commun. Signaling*, 2020, **18**(1), 46.

37 G. Jia and J. R. Sowers, Targeting endothelial exosomes for the prevention of cardiovascular disease, *Biochim. Biophys. Acta, Mol. Basis Dis.*, 2020, **1866**(8), 165833.

38 T. Romani de Wit, *et al.*, Real-time imaging of the dynamics and secretory behavior of Weibel-Palade bodies, *Arterioscler., Thromb., Vasc. Biol.*, 2003, **23**(5), 755–761.

39 C. Théry, Exosomes: secreted vesicles and intercellular communications, *F1000Prime Rep.*, 2011, **3**, 15.

40 D. D. Wagner, T. Mayadas and V. J. Marder, Initial glycosylation and acidic pH in the Golgi apparatus are required for multimerization of von Willebrand factor, *J. Cell Biol.*, 1986, **102**(4), 1320–1324.

41 S. R. Lentz and J. E. Sadler, Homocysteine inhibits von Willebrand factor processing and secretion by preventing transport from the endoplasmic reticulum, *Blood*, 1993, **81**(3), 683–689.

42 T. Minamino, I. Komuro and M. Kitakaze, Endoplasmic reticulum stress as a therapeutic target in cardiovascular disease, *Circ. Res.*, 2010, **107**(9), 1071–1082.

43 T. I. Ignashkova, *et al.*, [Deposition of von Willebrand factor in human endothelial cells HUVEC in the endoplasmic reticulum stress induced by an excess of homocysteine in vitro], *Patol. Fiziol. Eksp. Ter.*, 2012, **3**, 81–86.

44 M. A. Carew, E. M. Paleolog and J. D. Pearson, The roles of protein kinase C and intracellular Ca^{2+} in the secretion of von Willebrand factor from human vascular endothelial cells, *Biochem. J.*, 1992, **286**(Pt 2), 631–635.

45 Y. A. Miroshnikova, *et al.*, Calcium signaling mediates a biphasic mechanoadaptive response of endothelial cells to cyclic mechanical stretch, *Mol. Biol. Cell*, 2021, **32**(18), 1724–1736.

